Research Article

Journal of Environmental Nanotechnology

Photocatalytic Degradation Analysis of Rhodamine B and Eosin Yellow Dyes using Ag-doped TiO_2 Nanoparticles Synthesized *via* Sol-gel Method

R. Deepha and V. Senthilnathan*

Department of Physics, Chikkanna Government Arts College, Tirupur, TN, India

Received: 01.02.2026 Accepted: 24.02.2026 Published: 30.03.2026

*zndl.goyeo.nath.vasu@gmail.com

ABSTRACT

The sol-gel process was used to prepare Ag-doped TiO_2 nanoparticles with Ag concentrations of 1–5 mol%, which were then calcined for 3 hours at 500 °C. X-ray diffraction, field emission scanning electron microscopy with EDAX, and ultraviolet–visible spectroscopy were used to study the structural, morphological, and optical characteristics. Following Ag incorporation, the optical study showed improved light absorption and a notable decrease in band gap energy from 3.32 eV to roughly 2.00 eV. The degradation of Rhodamine B (RhB) and Eosin Yellow (EY) under UV light was used to measure the photocatalytic activity. The 5 mol% Ag-doped TiO_2 sample performed most effectively, reaching 99.07% degradation for EY and 98.15% for RhB. According to these results, a higher silver concentration enhances degradation by increasing light absorption and facilitating electron-hole separation. The incorporation of silver improves the photocatalytic activity of TiO_2 under UV irradiation.

Keywords: Ag-doped TiO_2 nanoparticles; Sol-gel process; Photocatalysis; Rhodamine B; Eosin Yellow.

1. INTRODUCTION

Nanoparticles play critical roles in many applications, and their formation, study, and use have recently attracted increasing attention from researchers (Huang *et al.* 2025). Because of their nanoscale structure and large numbers of active surface sites, semiconductor and metal oxide nanoparticles used in piezoelectric, optoelectronic, and sensing applications exhibit exceptional chemical and physical properties (Fujishima and Honda, 1972). Because of their high chemical stability, resistance to biodegradation, and potential toxicity, synthetic dyes from the textile, paper, leather, and chemical industries are particularly concerning as pollutants (Cardoso *et al.* 2021). The development of more effective and environmentally friendly treatment technologies is necessary because traditional wastewater treatment techniques (Mohamadpour *et al.* 2024), including adsorption, coagulation, and biological processes, often fail to fully mineralize these persistent pollutants. (Liang *et al.* 2017 and Mahdi *et al.* 2023)

Semiconductor-based photocatalysis has become a viable method for degrading organic contaminants by converting light energy into highly reactive species that mineralize complex chemical compounds into harmless end products (Ramesh *et al.* 2024; Balachandran *et al.* 2021). Excellent chemical stability, non-toxicity, low cost, and high oxidative potential make TiO_2 one of the most widely studied photocatalysts (Wang *et al.* 2012; Pawar *et al.* 2021). The broad band gap of TiO_2 (3.2 eV), which limits photoactivity primarily to the UV spectrum, and the rapid recombination of photogenerated electron–hole pairs, which drastically lowers photocatalytic efficiency, limit the material's practical use (Sen *et al.* 2005)

Silver doping has attracted interest because it can enhance light absorption and facilitate charge separation. However, few detailed studies have examined how varying amounts of silver affect the optical, structural, and photocatalytic properties of TiO_2 nanoparticles prepared by the sol-gel method. This study examines Ag-doped TiO_2 nanoparticles at various silver concentrations and assesses their ability to degrade Rhodamine B (RhB) and Eosin Yellow (EY) under UV light (Hossain *et al.* 2018). Titanium dioxide is commonly used in semiconductor photocatalysis to degrade organic dyes such as RhB and EY. This is because it has strong oxidative properties, is chemically stable, and is inexpensive (Lavorato *et al.* 2017). The present study focuses on the synthesis of pure and Ag-doped TiO_2 nanoparticles via the sol-gel method for photocatalytic applications (Jin *et al.* 2017; Liu *et al.* 2004; Bensouici *et al.* 2015). Rhodamine B and Eosin Yellow dyes were used in photocatalytic applications. Because of their distinct chemical structures and photophysical properties, EY and RhB are common test dyes for evaluating photocatalytic efficiency across a variety of organic pollutants. Eosin Yellow is an anionic dye widely used to dye silk, wool, and modified acrylic textiles for its vivid pinkish-red tone and superior

photostability (Ghime *et al*.2020). On the other hand, optical tracing, textiles, and cosmetics all extensively use RhB, a cationic synthetic dye. Analysing the degradation of both dyes improves understanding of the adsorption and photocatalytic processes occurring on the catalyst surface. Additionally, these dyes exhibit strong absorption in the visible wavelengths, making them suitable experimental materials for UV-visible spectral studies of photocatalytic removal. Thus, the photocatalytic efficiency of Ag-doped TiO_2 nanoparticles in removing organic pollutants from wastewater can be effectively evaluated using RhB and EY dyes (Sultana *et al.* 2023).

2. MATERIALS AND METHODS

2.1 Chemicals and Reagents

All chemicals used in this study were of analytical grade and employed without further purification. Titanium (IV) isopropoxide (97%) precursor and silver nitrate (>99%) ($AgNO_3$), used as the Ag dopant source, were obtained from Sigma-Aldrich Merck, Bangalore. Double-distilled water was used throughout the synthesis and photocatalytic experiments. Eosin Yellow and Rhodamine B dyes were selected as model organic pollutants to evaluate photocatalytic performance.

2.2 Experimental Design and Ag Doping Strategy

TiO_2 samples with 1, 2, 3, 4, and 5 mol% silver were prepared to reduce strong reaction effects and analyze a selection of doping levels. To ensure the precision of the results, every sample was prepared using the same method.

2.3 Synthesis of Pure TiO_2 Nanoparticles

Initially, 40 mL of ethanol was stirred for 10 minutes and then 29.606 mL of Titanium (IV) isopropoxide (TTIP) was added dropwise to the solvent at 1 mol%, and the mixture was stirred for 10 minutes. Afterwards, the mixture was continuously agitated while 10 mL of distilled water was added gradually. The mixture was then heated and kept at 50°C for 30 minutes. Hydrochloric acid was added dropwise over two hours, while continuously mixing the ingredients, to produce a milky-white solution with a pH of 3. This sol was aged for 10 hours and then dried in an oven at 100°C until all moisture was removed. The dried gel was manually crushed with a mortar and pestle. The product was then calcined for three hours at 500°C min^{-1} in a muffle furnace. The final TiO_2 particles were produced by grinding the white powder after the furnace cooled to room temperature (Kamrul *et al.* 2025).

2.4 Synthesis of Ag-Doped TiO_2 (1–5 mol%)

Silver nitrate solutions corresponding to 1 mol%, 2 mol%, 3 mol%, 4 mol%, and 5 mol% were dissolved in distilled water and added dropwise to the sol under stirring at 60°C for 2 hours. Ag nanoparticles were deposited on the TiO_2 surface. The gel was allowed to settle for 12 hours, washed with distilled water and acetone and then dried in an oven at 100°C until all moisture was removed. The dried gel was manually crushed with a mortar and pestle. The product was then calcined for 3 hours at 500 °C in a muffle furnace. The final Ag-doped TiO_2 particles were obtained by further grinding the light grey powder after the furnace had cooled to room temperature (Ghime *et al.* 2020).

2.5 Structural and Morphological Characterization

The crystalline structure and phase composition of pure and Ag-doped TiO_2 nanoparticles were analyzed using XRD with Cu Kα radiation. Diffraction patterns were recorded to identify phase purity and estimate crystallite size. Surface morphology and particle distribution were examined using FESEM. Energy-dispersive X-ray spectroscopy coupled with FESEM was employed to confirm elemental composition and quantify Ag incorporation.

2.6 Optical Characterization

UV–visible absorption spectra were recorded in the wavelength range 200–800 nm using a UV–visible spectrophotometer. Band gap energies were estimated from Tauc plots based on absorption data. The optical properties of pure TiO_2 were compared with those of Ag-doped TiO_2 to evaluate the influence of Ag incorporation on light absorption behavior.

2.7 Photocatalytic Activity

2.7.1 Selection of Model Pollutant

The photocatalytic activity of Ag-doped TiO_2 nanostructures in degrading RhB and EY dyes was evaluated under visible light.

2.7.2 Procedure for Photocatalytic Degradation

To prepare the stock solutions, 100 mg of each dye was dissolved in 1 L of double-distilled water, yielding a concentration of 100 mg/L. For photocatalytic experiments, 100 mL of the dye solution and 100 mg of photocatalyst were introduced into a cylindrical glass reactor to form a uniform suspension. The mixture was stirred with a magnetic stirrer in the dark for 30 minutes before exposure to light, allowing the dye and catalyst to reach adsorption-desorption equilibrium. Photocatalytic degradation was conducted under visible light from a 15

W lamp positioned 5 cm above the reactor. Stirring was maintained throughout the experiment to ensure homogeneous catalyst dispersion and consistent light exposure. At predetermined intervals, 3- to 5-mL samples were taken and left to settle. The clear liquid above the settled material was analyzed using a UV–Visible spectrophotometer (Cary 8454, Agilent, Singapore) to determine the residual dye concentration. Absorbance was measured at 560 nm for RhB and at 433 nm for EY (Mali *et al.* 2025; Kannan *et al.* 2025).

2.7.3 Degradation Efficiency Calculation

Photocatalytic degradation efficiency was calculated using:

$$\text{Degradation efficiency (\%)} = [(C_o - C_t) / C_o] \times 100,$$

where C_o and C_t represent the initial dye concentration and concentration at irradiation time t, respectively.

3. RESULTS AND DISCUSSION

3.1 Structural Analysis

Table 1. XRD analysis of pure and Ag-doped TiO_2 nanoparticles

Sample Code	Ag Content(mol%)	Crystallite Size, D(nm)
TTIP (Pure TiO_2)	0	34.48
TAg1%	1%	33.53
TAg2%	2%	32.39
TAg3%	3%	31.08
TAg4%	4%	30.91
TAg5%	5%	29.43

The crystalline structure and phase composition of pure and Ag-doped TiO_2 nanoparticles were investigated using X-ray diffraction analysis. The XRD patterns show that the prepared materials exhibit crystalline and structural phases, identified using a Pro Penalty CAL instrument with Cu Kα radiation (1.5406 Å). Fig. 1 shows Ag-doped TiO_2 nanoparticles at different concentrations (1%, 2%, 3%, 4%, and 5%). In the XRD pattern of pure TiO_2 and Ag-doped TiO_2 NPs, the diffraction peaks corresponding to the (101), (004), (200), (105), (116), and (204) crystallographic planes confirm the tetragonal rutile phase of TiO_2, in good agreement with JCPDS No. 21-1276. The respective values are in accordance with standard rutile TiO_2 data (Deng *et al.* 2023). The crystalline size was calculated by using Scherrer's formula.

$$D = K\lambda/\beta\cos\theta,$$

where λ is the wavelength of the X-ray beam, θ is the diffraction angle, D-crystallite size, K is the shape factor, and β is the full width at half maximum of the peak.

Reducing the crystalline size and adding Ag both improve charge separation and light absorption, thereby increasing photocatalytic activity (Gupta *et al.* 2013). Since both pure and Ag-doped samples show the same diffraction peaks, Ag does not change the crystal structure of TiO_2.

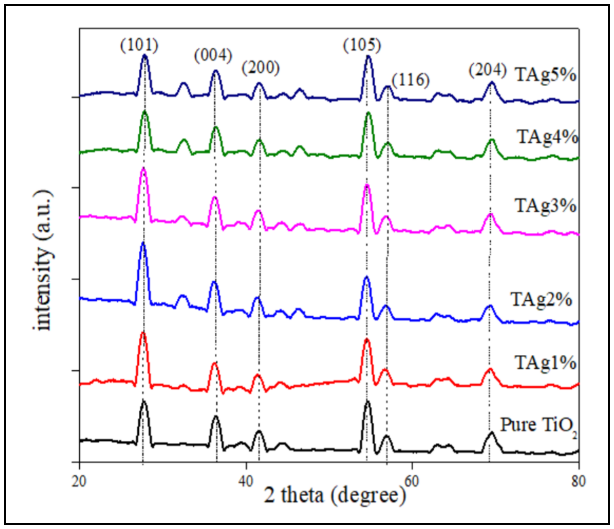


Fig. 1: XRD analysis of pure TiO_2, TAg1%, TAg2%, TAg3%, TAg4% and TAg5%

3.2 Morphological and Elemental Analysis (FESEM and EDAX)

Field-emission scanning electron microscopy was employed to study the surfaces of pure and Ag-doped TiO_2 nanoparticles. Most of the nanoparticles appeared nearly spherical and were evenly distributed. Particle size was measured from FESEM micrographs using image analysis software (ImageJ) by randomly selecting particles across multiple fields of view. The particle size distribution was determined by calculating the mean particle size. Measurements from images with 100-200 nm scale bars showed that increasing the amount of Ag reduced particle size. The average sizes of pure and Ag-doped TiO_2 were 28.28 nm, 26.06 nm, 23.58 nm, 22.37 nm, 20.58 nm, and 19.75 nm (Wang *et al.* 2012). Previous studies reported similar morphological characteristics and particle-size reductions in Ag-modified TiO_2 systems. Metal doping affected nucleation and crystal growth during synthesis, resulting in smaller nanoparticles and improved photocatalytic activity (Pawar *et al.* 2021).

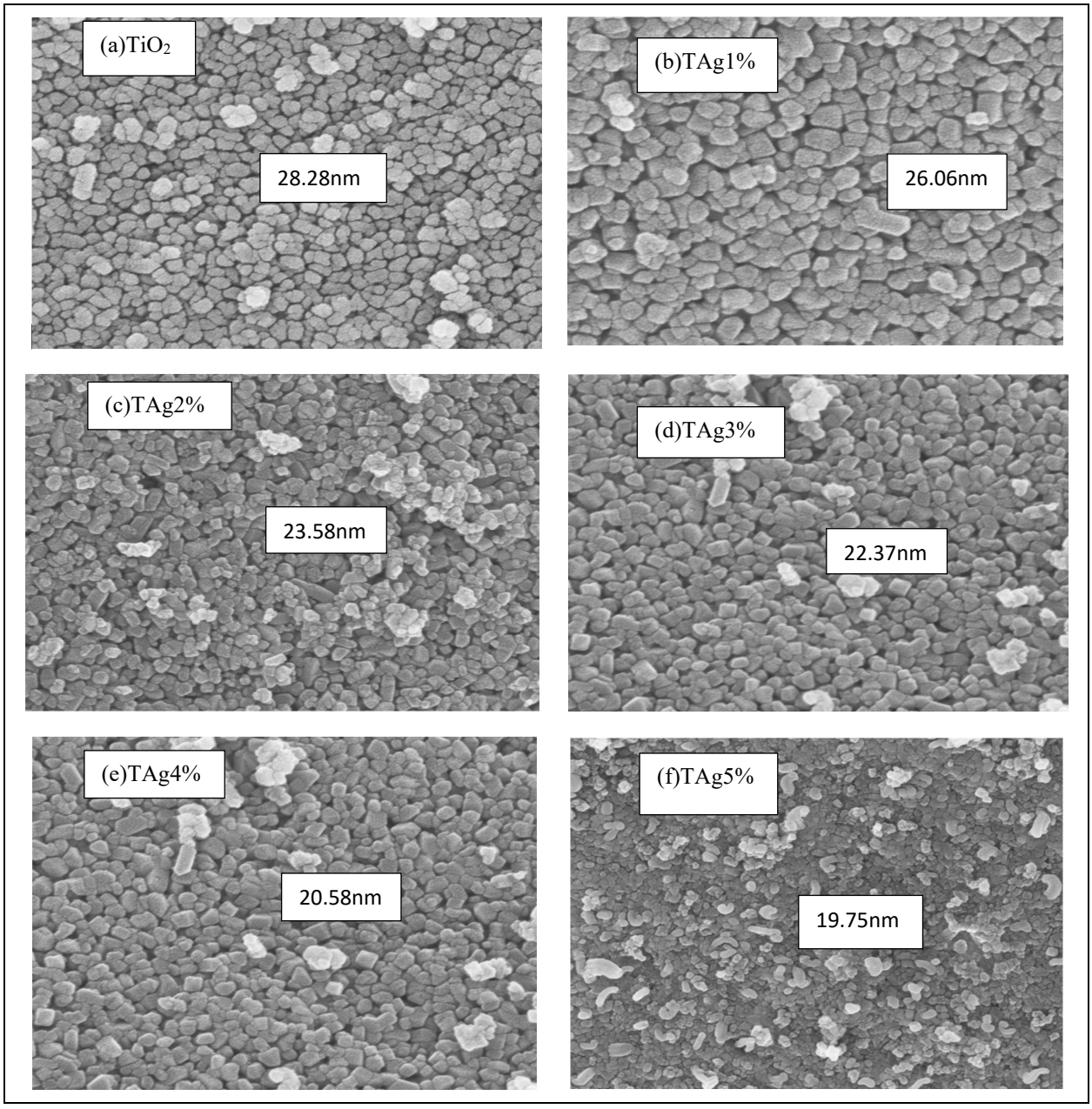
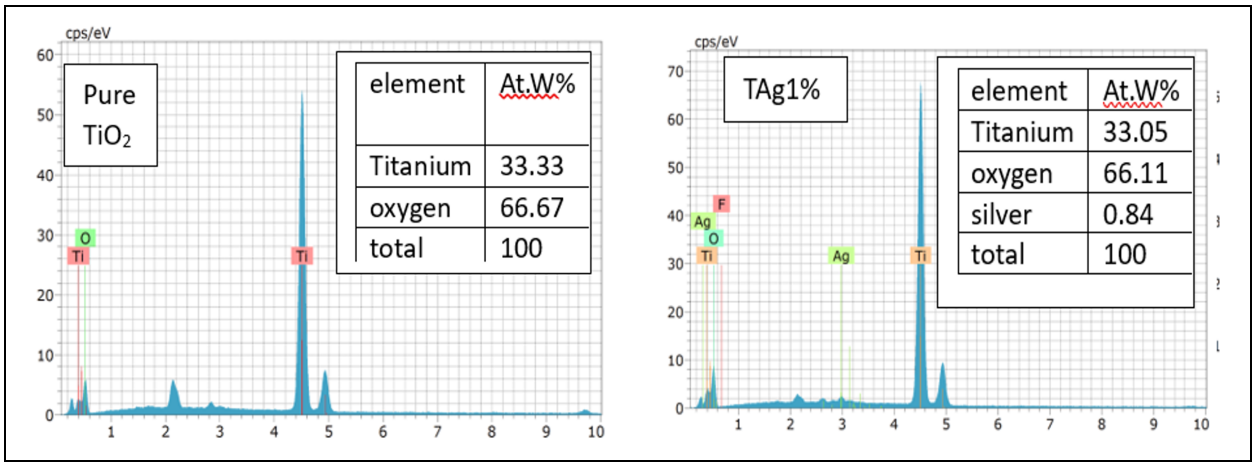


Fig. 2: The FESEM images of pure TiO2 and TAg1%, TAg2%, TAg3%, TAg4%, TAg5%



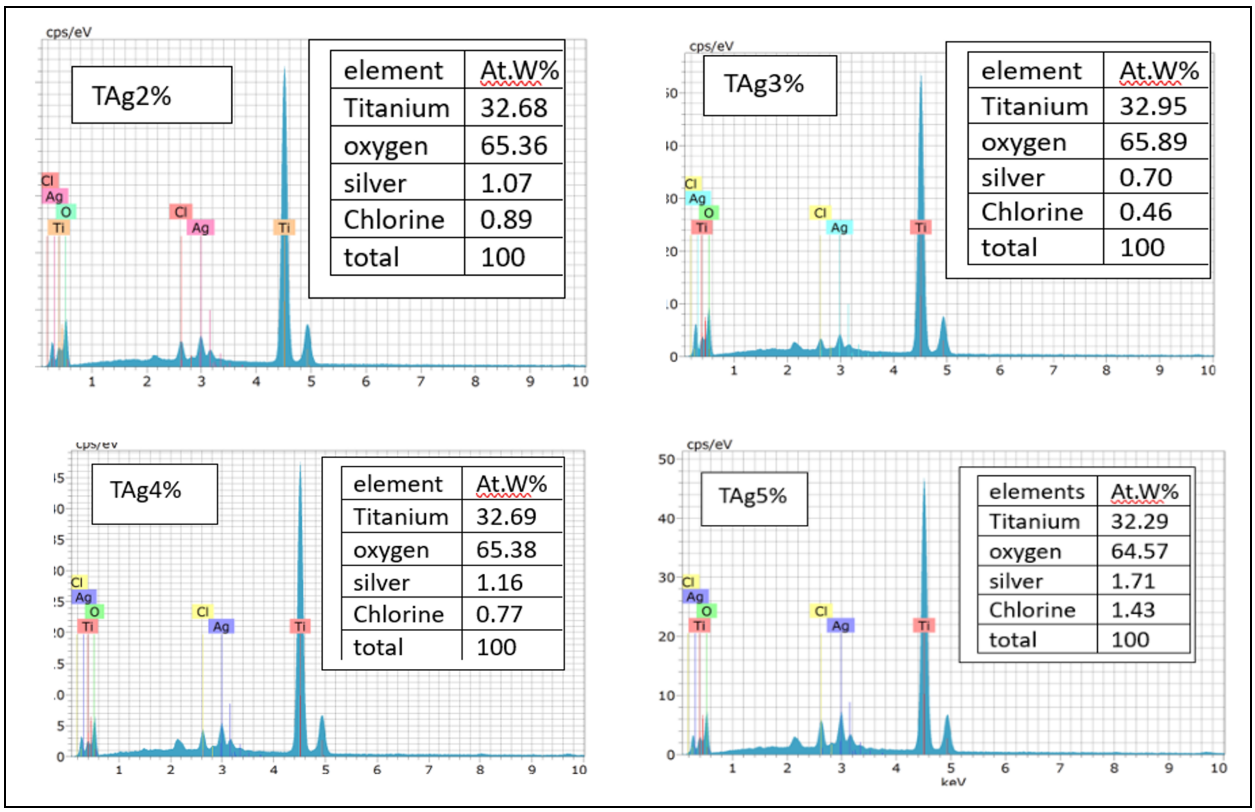


Fig. 3: EDAX and atomic weight% analysis of pure TiO_2 and doped TAg 1%,2%,3%,4%,5 mol%

The elemental composition of both pure and Ag-doped TiO_2 nanoparticles was determined using energy-dispersive X-ray analysis. Only the peaks for Ti and O are seen in the EDAX spectrum of the pure TiO_2 sample, showing that no impurities are present during the formation of TiO_2. The presence of additional peaks for silver in the EDAX spectra of Ag-doped TiO_2 samples indicates successful incorporation of Ag into the TiO_2 material. Ag was shown to enhance photocatalytic performance by improving electron-hole separation and increasing ultraviolet light absorption (Lee *et al.* 2020)

3.3 Optical Properties (UV–visible Spectroscopy)

The UV–visible absorption spectra of pure and Ag-doped TiO_2 nanoparticles were recorded in the wavelength range 200–800 nm to evaluate the influence of silver incorporation on the optical properties of the material. The spectrum of pure TiO_2 exhibits strong absorption in the ultraviolet region, with a sharp absorption edge around 380–390 nm, corresponding to the intrinsic band-gap transition of TiO_2. This absorption behaviour is characteristic of wide-band-gap semiconductor materials and confirms the formation of phase-pure TiO_2.

The absorption coefficient (α) formed by UV-Vis absorption measurements was used to calculate the optical band gap of pure and Ag-doped TiO_2 nanoparticles. The following formula was used for calculating the absorption coefficient:

$$\alpha=2.303A/d,$$

where d is the optical path length, and A is the sample's absorbance. Additionally, Tauc plots were used to determine the optical band gap energy of both pure and Ag-doped TiO_2. The absorption coefficient and photon energy are related in the following way:

$$(\alpha h\nu)^2 = A(h\nu - E_g),$$

where h is Planck's constant (6.626×10^{-31} Js), ν is the incident photon frequency, α is the absorption coefficient, and A is a parameter relating to the effective mass associated with the valence and conduction bands. The linear region of the $(\alpha h\nu)^2$ vs. hν plot was used to determine the band gap energy. The band gap values for pure and Ag-doped TiO_2 nanoparticles were calculated using these Tauc plots. Pure and Ag-doped TiO_2 nanoparticle band gap values were calculated. The synthesis material's optical energy was TiO_2 and TAg (1–5 mol%). From 3.32 eV to 3.03 eV, 2.79 eV, 2.69 eV, 2.02 eV, and 2.00 eV, the corresponding band gap energy decreased. (Gupta *et al.* 2013).

The surface plasmon resonance (SPR) effect of metallic silver nanoparticles is responsible for increased absorption in the visible range, a trend that becomes more pronounced with increasing Ag concentration. (Mahdi *et al.* 2023). These optical changes facilitate more efficient generation and separation of charge carriers under UV

irradiation, which directly contributes to the improved photocatalytic degradation performance observed for RhB and EY dyes (Sen *et al*. 2005).

3.4 Rhodamine B and Eosin Yellow Dye Degradation Studies

The full-scan UV–visible absorption spectra of RhB and EY at pH 3 during the photocatalytic studies are shown in Figures 4 and 5. The efficiency of pure TiO_2 and Ag-doped TiO_2 nanoparticles (1–5 mol% Ag) in the degradation of Rhodamine B (RhB) and Eosin Yellow (EY) under identical UV radiation conditions was examined in this study (Deng *et al*. 2019). UV–visible spectrophotometry was used to measure dye concentrations at 433 nm for EY and at 560 nm for RhB (Sultana *et al.* 2023). The photocatalytic degradation efficiencies of both dyes were calculated using the same methods.

The results show that adding silver to the TiO_2 structure increases the degradation efficiency of RhB. Pure TiO_2 achieves about 60.34% degradation after 150 minutes of irradiation, but adding silver significantly improves its photocatalytic performance. The 5 mol% Ag-doped TiO_2 sample performs best, reaching about 98.15% degradation of RhB. This suggests that silver doping helps separate photogenerated electron-hole pairs and reduces charge recombination. A similar pattern appears in the degradation of EY dye. Pure TiO_2 achieves about 74.74% degradation in 120 minutes, faster than with RhB. This improved performance may be due to the EY molecular structure, which helps it adhere more strongly to the catalyst and makes it easier to break its molecular rings. As Ag content increases, degradation efficiency rises steadily to 79.30%, 83.03%, 89.08%, 92.37%, and 99.07% for TiO_2 doped with 1%, 2%, 3%, 4%, and 5% Ag, respectively. The 5% Ag-doped TiO_2 sample removes EY almost completely in a shorter time. The overall photocatalytic process for both dyes is the same; EY shows higher degradation efficiency with pure TiO_2 than RhB. The surface plasmon interaction of Ag nanoparticles enhances light absorption and facilitates efficient hole-driven oxidation during photocatalysis, thereby increasing activity with Ag doping (Krejčíková *et al.* 2012). When exposed to light, Ag-modified TiO_2 absorbs photons with energy equal to or greater than its band gap. This process moves electrons from the valence band to the conduction band, leaving behind holes in the valence band. The absorbed electrons react with dissolved oxygen to produce superoxide radicals ($\bullet O_2^-$), while the holes react with water molecules or hydroxide ions to form hydroxyl radicals (•OH). As a result, the organic dye molecules are broken down into CO_2 and H_2O (Zarzzeka *et al.* 2024).

3.4.1 Photocatalytic Reaction Equation:

Light excitation:

$$TiO_2 + hv + e^-(CB) + h^+(VB) \quad \ldots (1)$$

Electron Trapping by Ag:

$$Ag + e^- \rightarrow Ag^- \quad \ldots (2)$$

Superoxide Radical Formation:

$$O_2 + e^- \rightarrow (\bullet O_2^-) \quad \ldots (3)$$

Hydroxyl Radical Formation:

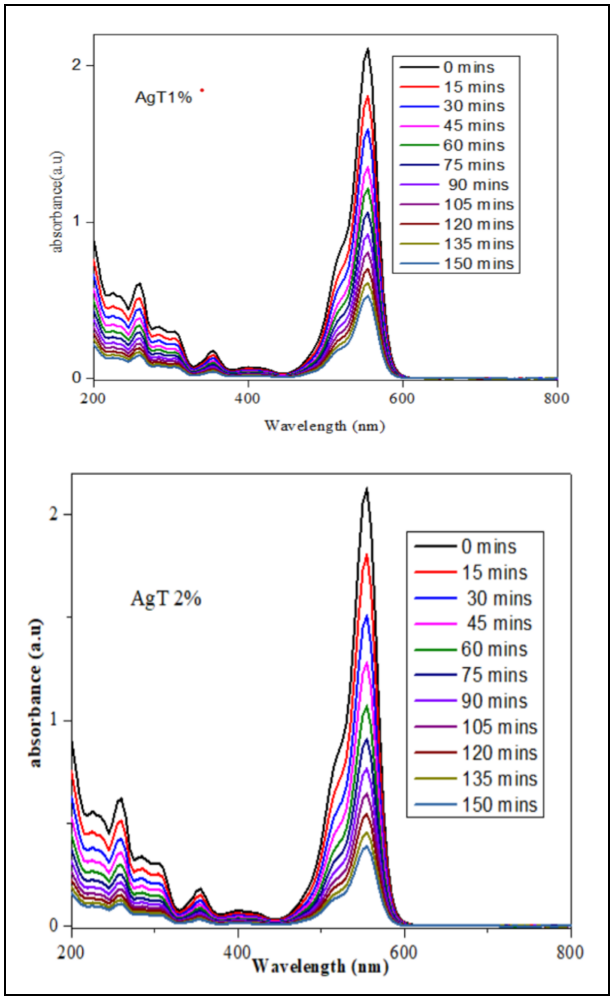
$$h^+ + H_2O \rightarrow \blacksquare OH + H^+ \quad \ldots (4)$$

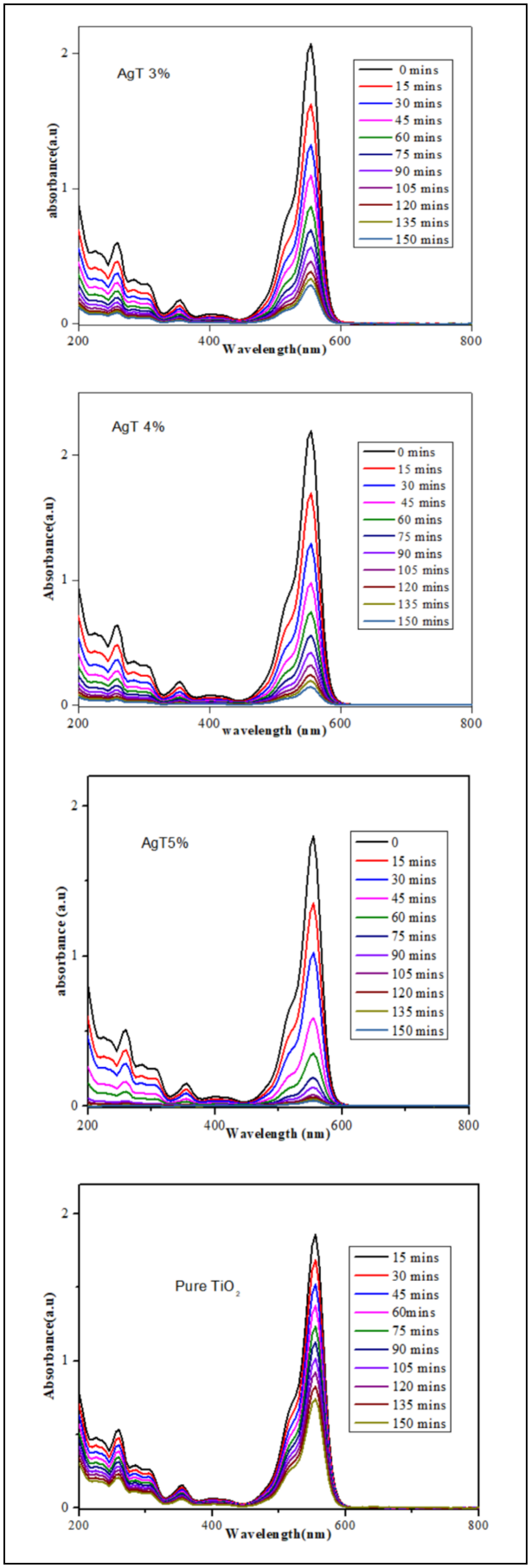
$$h^+ + H_2O \rightarrow \blacksquare OH \quad \ldots (5)$$

Dye Degradation:

$$RhB + \blacksquare OH \rightarrow CO_2 + H_2O + \text{Inorganic acid} \quad \ldots (6)$$

$$EY + \blacksquare OH \rightarrow CO_2 + H_2O + \text{Inorganic acid} \quad \ldots (7)$$





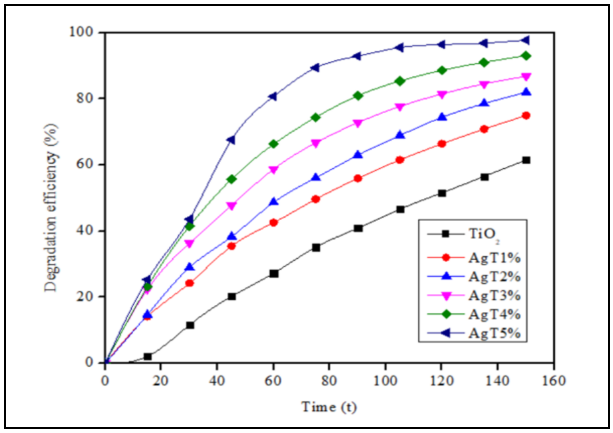
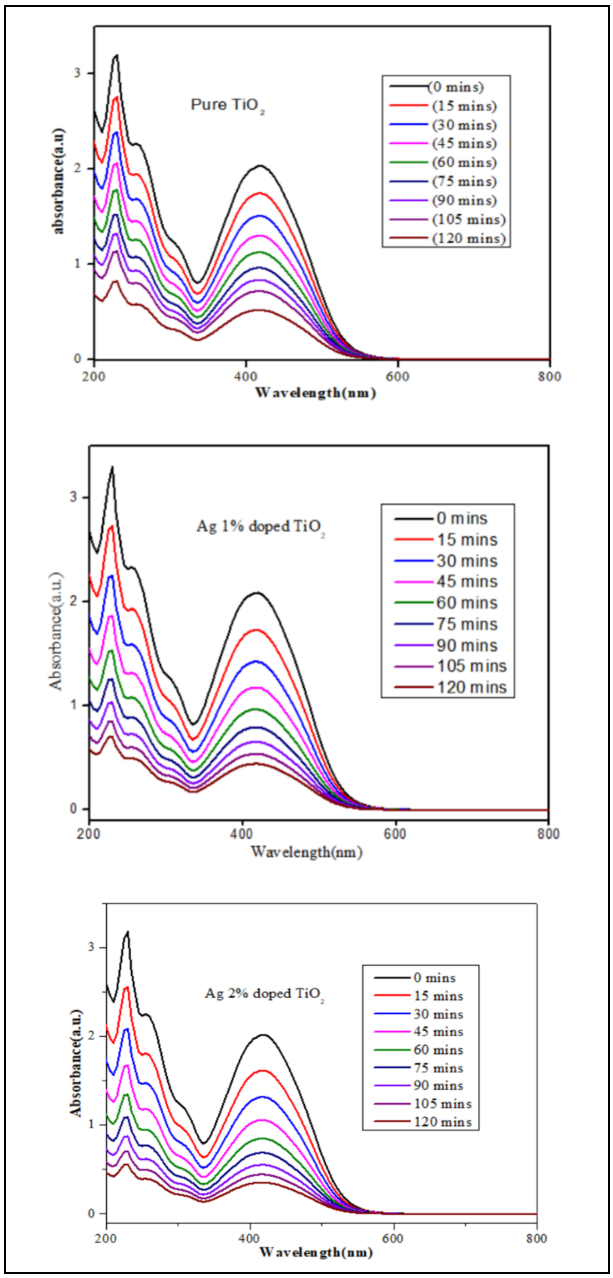


Fig. 4: The time-dependent UV-vis absorption spectra of eosin yellow dye degradation



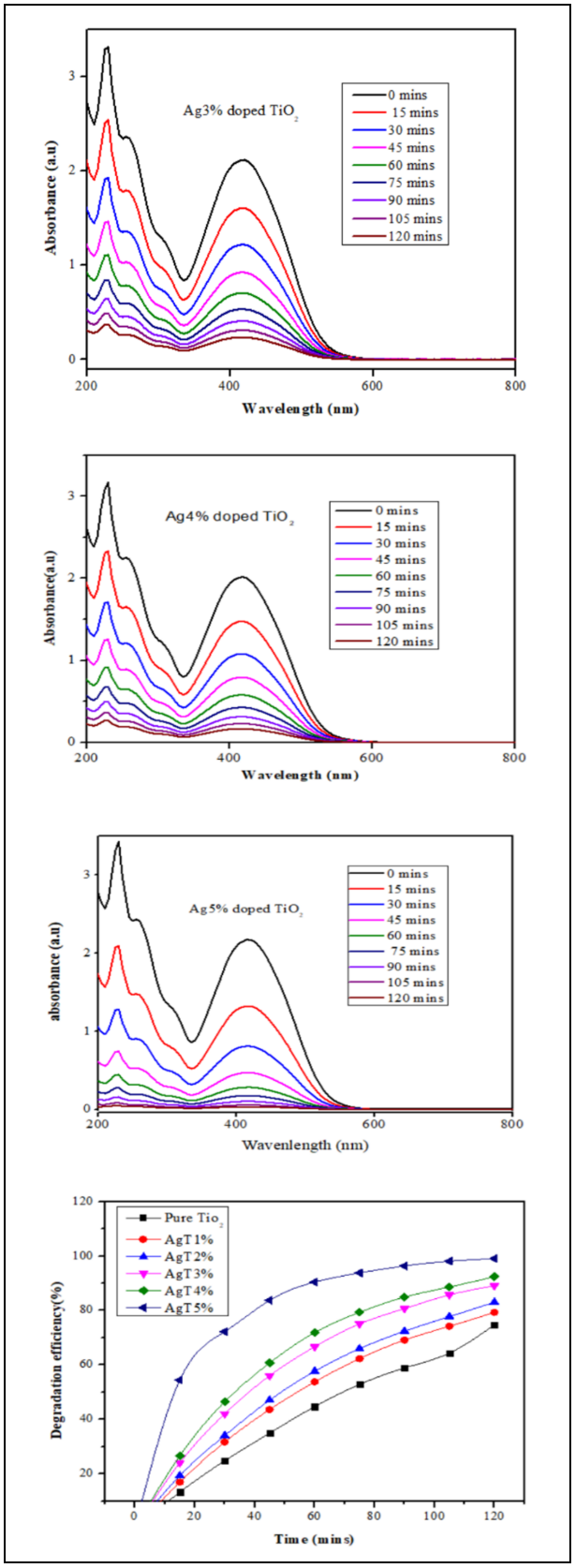


Fig. 5: Time-dependent UV-vis absorption spectra of eosin yellow dye degradation

Table 3: Time-dependent UV-Vis absorption spectra of RhB and EY dyes degradation

S. NO.	Sample Name	Dye Used	Degradation Efficiency (%)	Dye Used	Degradation Efficiency (%)
1.	Pure TiO_2	RhB	60.34%	EY	74.74%
2.	AgT1%	RhB	75.36%	EY	79.30%
3.	AgT2%	RhB	81.96%	EY	83.03%
4.	AgT3%	RhB	86.23%	EY	89.08%
5.	AgT4%	RhB	92.98%	EY	92.37%
6.	AgT5%	RhB	98.15%	EY	99.07%

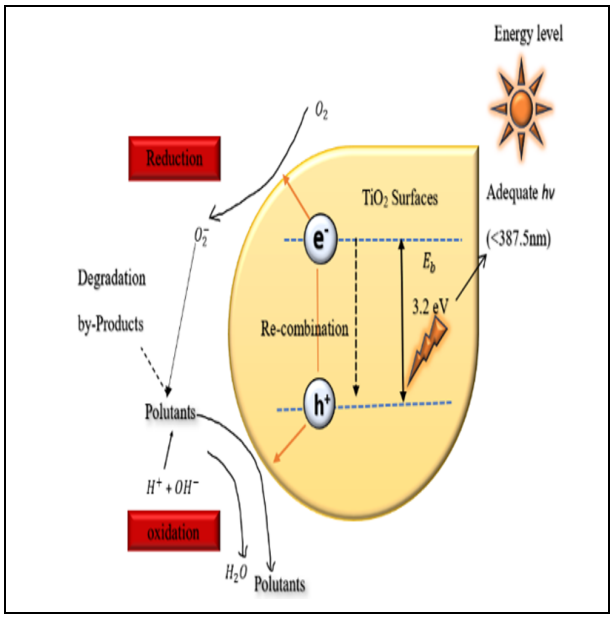


Fig. 6: Schematic representation of the photocatalytic activity of Ag-doped TiO_2 nanoparticles using RhB and EY degradation

4. CONCLUSION

Ag-doped TiO_2 nanoparticles containing 1–5 mol% Ag were synthesized using the sol–gel method and exhibited enhanced photocatalytic activity. Specifically, X-ray diffraction analysis indicated that the rutile phase was predominant, while the crystallite size decreased with increasing Ag concentration. Furthermore, optical characterization revealed improved light absorption following Ag incorporation. As a result, photocatalytic analysis under ultraviolet irradiation indicated that the degradation efficiency of RhB and EY increased with increasing Ag concentration, with 5 mol% Ag-doped TiO_2 achieving the highest removal efficiency. This improved performance is likely due to improved charge-carrier separation and increased light absorption, suggesting that Ag-doped TiO_2 could be useful for wastewater treatment.

FUNDING

This research received no specific grant from any funding agency in the public, commercial, or not-for-profit sectors.

CONFLICTS OF INTEREST

The authors declare that there is no conflict of interest.

COPYRIGHT

This article is an open-access article distributed under the terms and conditions of the Creative Commons Attribution (CC BY) license (http://creativecommons.org/licenses/by/4.0/).

REFERENCE

Balachandran, K., Vijayakumar, G., Mageswari, S., Preethi, A. and Viswak, S. M. S., Synthesis and Characterization of Ag-decorated TiO_2 Nanoparticles for Photocatalytic Application, *J. Environ. Nanotechnol.,* 10(4), 13-18 (2021) https://doi.org/10.13074/jent.2021.12.14446

Bensouici, F., Souier, T., Dakhel, A. A., Iratni, A., Tala-Ighil, R. and Bououdina, M., Synthesis, characterisation, and photocatalytic behaviour of Ag-doped TiO_2 thin film, *Superlatt. Microstruct*., 85, 255-265 (2015). https://doi.org/10.1016/j.spmi.2015.05.028

Cardoso, I. M. F., Cardoso, R. M. F. and Esteves da Silva, J. C. G., Advanced oxidation processes coupled with nanomaterials for water treatment, *Nanomater.*, 11(8), 2045(2021). https://doi.org/10.3390/nano11082045.

Deng, H., He, H., Sun, S., Zhu, X., Zhou, D., Han, F., Bin, H. and Pan, X., Photocatalytic degradation of dye by Ag/TiO_2 nanoparticles prepared with different sol–gel crystallization in the presence of effluent organic matter, *Environ. Sci. Pollut. Res*., 26,35900-35912(2019). https://doi.org/10.1007/s11356-019-06728-0

Fujishima, A. and Honda, K., Electrochemical Photolysis of Water at a Semiconductor Electrode, *Nat.,* 238, 37-38(1972). https://doi.org/10.1038/238037a0

Ghime, D., Mohapatra, T., Verma, A., Banjare, V. and Ghosh, P., Photodegradation of aqueous eosin yellow dye by carbon-doped TiO_2 photocatalyst, *IOP Conf. Series: Earth Environ. Sci.*, 597(1), 012010(2020). https://doi.org/10.1088/1755-1315/597/1/012010

Gupta, K., Singh, R. P., Pandey, A. and Pandey, A., Photocatalytic antibacterial performance of TiO_2 and Ag-doped TiO_2 against *S. Aureus. P. Aeruginosa and E. Coli*, *Beilstein J. Nanotechnol.,* 4(1), 345–351(2013). https://doi.org/10.3762/bjnano.4.40

Hossain, M. A., Elias, M., Sarker, D. R., Diba, Z. R., Mithun, J. M., Azad, M. A. K., Ahmed, I. S., Rahman, M. M., Jamal, U. M. and Uddin, N., Synthesis of Fe- or Ag-doped TiO_2–MWCNT nanocomposite thin films and their visible-light induced catalysis of dye degradation and antibacterial activity, *Res. Chem. Intermed.*, 44, 2667-2683(2018). https://doi.org/10.1007/s11164-018-3253-z

Huang, K. E. D., Lai, C. W., Juan, J. C., Pang, Y. L., Khe, C. S., Badruddin, I. A., Gapsari, F. and Anam, K., Recent advances in titanium dioxide bio-derived carbon photocatalysts for organic pollutant degradation in wastewater, *iSci.*, 28(5), 112368(2025). https://doi.org/10.1016/j.isci.2025.112368

Jin, C., Dai, Y., Wei, W., Ma, X., Li, M. and Huang, B., Effects of single metal atom (Pt, Pd, Rh, and Ru) adsorption on the photocatalytic properties of anatase TiO_2, *Appl. Surf. Sci.,* 426, 639-646(2017). https://doi.org/10.1016/j.apsusc.2017.07.065

Kamrul, M. H., Hossain, M. M., Faisal, I. C., Islam. R., Rahan, I. and Akhtar, S., Synthesis and characterization of Ag-doped TiO2 nanoparticle and evaluation of its photocatalytic activity in the degradation of p-nitrophenol, *Next Nanotechnol.,* 8, 100272(2025). https://doi.org/10.1016/j.nxnano.2025.100272

Kannan, P., Surumbarkuzhali, N., Surendhiran, S., Naren Vidaarth, T. M. and Sneha, M., Synergistic visible light-driven and persistent photocatalytic activity of morphology-engineered vanadium nanostructures, *J. Ind. Chem. Soc*., 102(12), 102214(2025). https://doi.org/10.1016/j.jics.2025.102214

Krejčíková, S., Matějová, L., Kočí, K., Obalová, L., Matěj, Z., Čapek, L. and Šolcová, O., Preparation and characterisation of Ag-doped crystalline titania for photocatalysis applications, *Appl. Catal. B: Environ*., 111–112, 119–125 (2012). https://doi.org/10.1016/j.apcatb.2011.09.024

Lavorato, C., Argurio, P., Mastropietro, T. F., Pirri, G., Poerio, T. and Molinari, R., Pd/TiO_2 doped faujasite photocatalysts for acetophenone transfer hydrogenation in a photocatalytic membrane reactor, *J. Catal*., 353, 152-161(2017). https://doi.org/10.1016/j.jcat.2017.07.015

Lee, S. Y., Kang, D., Jeong, S., Do, H. T. and Kim, J. H., Photocatalytic Degradation of Rhodamine B Dye by TiO_2 and Gold Nanoparticles Supported on a Floating Porous Polydimethylsiloxane Sponge under Ultraviolet and Visible Light Irradiation, *ACS Omega*, 5(8), 4233–4241(2020). https://doi.org/10.1021/acsomega.9b04127

Liang, H., Jia, Z., Zhang, H., Wang, X. and Wang, J., Photocatalysis oxidation activity regulation of Ag/TiO_2 composites evaluated by the selective oxidation of Rhodamine B, *Appl. Surf. Sci.*, 422, 1–10(2017). https://doi.org/10.1016/j.apsusc.2017.05.211

Liu, S. X., Qu, Z. P., Han, X. W. and Sun, C. L., A mechanism for enhanced photocatalytic activity of silver-loaded titanium dioxide, *Catal. Today*, 93-95, 877-884 (2004). https://doi.org/10.1016/j.cattod.2004.06.097

Mahdi, Z. S., Aljeboree, A. M., Rasen, F. A., Salman, N. A. A. and Alkaim, A. F., Synthesis, Characterization, and Regeneration of Ag/TiO_2 Nanoparticles: Photocatalytic Removal of Mixed Dye Pollutants, *Eng. Proce.*, 59(1), 216(2023). https://doi.org/10.3390/engproc2023059216

Mali, D. G., Patil, S. P., Sonawane, G. H., Bhadane, B. S. and Mahajan, V. K., Synthesis of TiO_2 and Ag/Cu doped TiO2 nanoparticles in a green approach and assess their structural, morphological, and photocatalytic applications, *Hybrid Adv.,* 10, 100468(2025). https://doi.org/10.1016/j.hybadv.2025.100468

Mohamadpour, F. and Amani, A. M., Photocatalytic systems: reactions, mechanisms, and applications, *RSC Adv.,* 14(29), 20609–20645(2024). https://doi.org/10.1039/d4ra03259d

Pawar, M. J., Nimbalkar, V. B., Khajone, A. D. and Deshmukh, S. B., Ag-Doped TiO_2: Synthesis, Characterization and Photodegradation of 4BS Dye, *J. Nanosci. Technol.*, 7(4), 952–955(2021). https://doi.org/10.30799/jnst.328.21070401

Ramesh, N., Lai, C. W., Johan, M. R. bin, Mousavi, S. M., Badruddin, I. A., Kumar, A., Sharma, G. and Gapsari, F., Progress in photocatalytic degradation of industrial organic dye by utilising the silver-doped titanium dioxide nanocomposite, *Heliyon*, 10(24), e40998(2024). https://doi.org/10.1016/j.heliyon.2024.e40998

Sen, S., Mahanty, S., Roy, S., Heintz, O., Bourgeois, S. and Chaumont, D., Investigation on sol-gel synthesized Ag-doped TiO_2 cermet thin films, *Thin Solid Films*, 474(1–2), 245–249(2005). https://doi.org/10.1016/j.tsf.2004.04.004

Sultana, R., Liba, S. I., Rahman, M. A., Yeachin, N., Syed, I. M. and Bhuiyan, M. A., Enhanced photocatalytic activity in RhB dye degradation by Mn and B co-doped mixed-phase TiO_2 photocatalyst under visible light irradiation, *Surf. Interf.*, 42, 103302(2023). https://doi.org/10.1016/j.surfin.2023.103302

Wang, R. Wang, P. Yu, H. and Yu, J., UV- and visible-light photocatalytic activity of simultaneously deposited and doped Ag/Ag(I)-TiO_2 photocatalyst, *J. Phy. Chem. C*, 116(33),17721,17728(2012). https://doi.org/10.1021/jp305774n

Zarzzeka, C., Goldoni, J., de Paula de Oliveira, J. do R., Lenzi, G. G., Bagatini, M. D. and Colpini, L. M. S., Photocatalytic action of Ag/TiO2 nanoparticles to emerging pollutants degradation: A comprehensive review, *Sustain. Chem. Environ.,* 8, 100177(2024). https://doi.org/10.1016/j.scenv.2024.100177